Characterization and Mechanical Property Measurements by Instrumented Indentation Testing of Niger Delta Oil Shale Cuttings

*Ifeanyi Emmanuel Kalu[1,2,a], Ericmoore Jossou[3,b], Emmanuel Kwesi Arthur[4,c], Simon Ja'afaru[1,d], Edith Yohanna Ishidi.[1,e]

[1]Polymers and Advanced Composites Department, Sheda Science and Technology Complex, FCT, Nigeria
[2]Mechanical and Aeronautical Engineering Department, University of Pretoria, Pretoria, South Africa
[3]Mechanical Engineering Department, University of Saskatchewan, Saskatoon, S7N 5A9, Saskatchewan, Canada.
[4]Materials Engineering Department, Kwame Nkrumah University of Science and Technology, Kumasi, Ghana.
[a]u15327206@tuks.co.za, [b]ericmoore.jossou@usask.ca, [c]ekarthur.coe@knust.edu.gh, [d]simonjaf@gmail.com, [e]ogbosoedith@gmail.com.

Abstract

Oil shales have unstable mechanical and chemical properties, which makes their extraction for characterization and conventional mechanical testing uneasy and complex. Most often, mechanical property measurements are usually taken from core samples that are costly to extract and test using conventional testing methods. This paper presents a focused study carried out on oil shale cuttings obtained from the sidewalls of two different wellbore depths in the Niger Delta area of Nigeria. Using the X-ray Diffraction (XRD) and Scanning Electron Microscope (SEM) characterization techniques, the morphology of these shales was studied. The results obtained clearly showed the composition, bonding and variations in the morphology of the studied shale samples. Furthermore, the heterogeneity associated with these shales across varied depths were revealed. An efficient and less expensive technique compared to conventional testing methods, instrumented indentation testing (IIT) was carried out to obtain essential mechanical parameters of the shale specimen. These properties are important parameters in determining the hydrocarbon storage space of shale formations, wellbore stability, and optimization of hydraulic fracturing which is necessary for efficient drilling operations.

Keywords: Oil shale cuttings, characterization, mechanical testing, XRD, SEM, Instrumented Indentation Testing, Niger Delta.

1 Introduction

Shales are granulated sedimentary rock particles, essentially made up of minerals such as clay, quartz and other minerals. Sedimentary rocks that are rich in organic matter (kerogen) and can produce oil when they undergo process of pyrolysis, hydrogenation or thermal dissolution are typically referred to as oil shales [1]. These shales make up more than 75% of drilled formations, as such hold vast natural oil and gas resources [2–4]. They are responsible for at least 90% of wellbore stability problems, which are the primary cause of financial losses in boreholes in the drilling industry [2,3]. As such, the measurement of shale properties are essential to elucidate their strength and behavior under extreme conditions, and as such enhance wellbore stability [2,5,6]. Mechanical features of shales are also essential parameters for the modeling of basins, seismic response interpretation and for drilling optimization. [5,6] Equally, these properties of shales, mainly the elastic modulus, hardness and compressive strength are useful for determining their storage space, rate of penetration, wellbore ability, and optimizing hydraulic fracturing in unconventional reservoirs, which enhances the production of hydrocarbons from such wells [7–14].

Generally, shales are not as permeable compared to other reservoir rocks due to the varied structure and composition especially at small scales [8–11,15,16]. The characterization of shale is not only complicated but also challenging because of the heterogeneity it exhibits. Across different depths and locations, oil shales have showed varied physical and microstructural features [8–12,15–18]. Hence, focused study of oil shales based on their locations is relevant to understanding their micro- and nano structural properties.

Due to the structural variability of these shales, they have irregular mechanical and chemical properties, which makes their extraction for mechanical characterization, arduous and complicated [4,6,11,19]. Measurement techniques normally used to evaluate shale mechanical parameters are: standard rock uni-axial/tri-axial testing carried out on core samples, wave velocity method, and acoustic or wireline logging [2,5,6,19,20]. Also, due to their structural variability, core samples used for the standard mechanical test are quite expensive to extract from their wellbores and could often be difficult to obtain samples that will be suitable for the test [5,6,14,19]. To overcome these draw backs, Instrumented Indentation Testing (IIT); a method for evaluating the mechanical features of small volumes of materials, developed by Oliver and Pharr [21,22], which was an extension of previous works done by Pethica, et al. [23] and Doerner and Nix [24], can now be used to obtain the mechanical parameters of shales.

Within the Niger Delta oil-rich region of Nigeria, research conducted have been focused around sedimentation studies [25–27], reservoir description and characterization [27–30], and petrophysical and lithology properties [26,31]. No studies known to the authors have been conducted on the Niger Delta oil shale cuttings using IIT. This paper provides extended insights on shale properties that could be useful for further development of this oil rich region in Nigeria. Outcomes of studies on structural characterization and mechanical property measurements using IIT of oil shale cuttings extracted from two different depths in the Niger Delta area of Nigeria are hereby reported.

2 Instrumented Indentation Testing (IIT)

IIT is an improved technique of conventional hardness tests, which include Rockwell, Vickers, Knoop, and Brinell. It shares some similarity with these conservative test methods in that the rigid indenter, normally diamond, is thrust into contact with the sample to be tested. Whereas the conventional hardness methods gives only one deformation measurement in response to an applied force, the force and penetration depth of IIT are measured for the full range of the period that the indenter stays on the test specimen [22,32]. IIT involves the mechanical probing of a material surface using an indenter with a defined geometry and mechanical parameters. This creates an indentation at a nanoscale within the sample, with the constantly changing load and penetration depths measured simultaneously. With this method, mechanical features of materials evaluated at miniature scales can be achieved through proper data analysis of the load-displacement curve obtained from an accurate indentation of the material. Fig. 1 shows a schematic illustration of how the IIT is to be conducted while Fig. 2 illustrates the generation of a load-displacement curve from a conducted test.

Fig. 1 shows a force, F applied by the indenter on the exterior of the sample up until it makes a contact with the sample at h_c. The indenter is held within the sample for 3-5 secs, after which it is unloaded. This leads to the formation of a loading and unloading profile over the entire displacement depth created by the indenter, corresponding to the sample surface, h. Due to the unloading of the indenter from the sample, recovery of the elastic displacement occurs, which creates a permanent depth of penetration, h_p in the sample after it has been fully unloaded. Fig. 2 shows that the indenter penetrates the sample up to when a maximum force (F_{max}) is achieved at a maximum displacement, h_{max}. This displacement corresponds to the location of the first contact made by the indenter on the sample surface. The indenter is held at F_{max} to minimize relaxation effects, after which it is pulled back from the specimen at the same loading rate. The depth at which the indenter tip makes a final contact on the sample after it is fully withdrawn is seen as h_p and the elastic unloading stiffness is expressed as $S = dF/dh$.

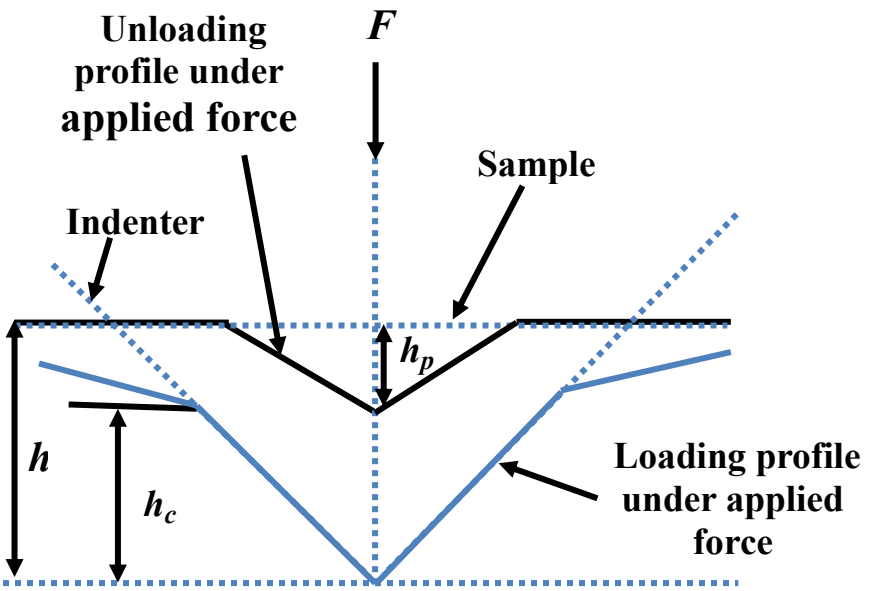

Fig. 1. Schematic representation of an instrumented indentation test adapted from Ref. [11,22].

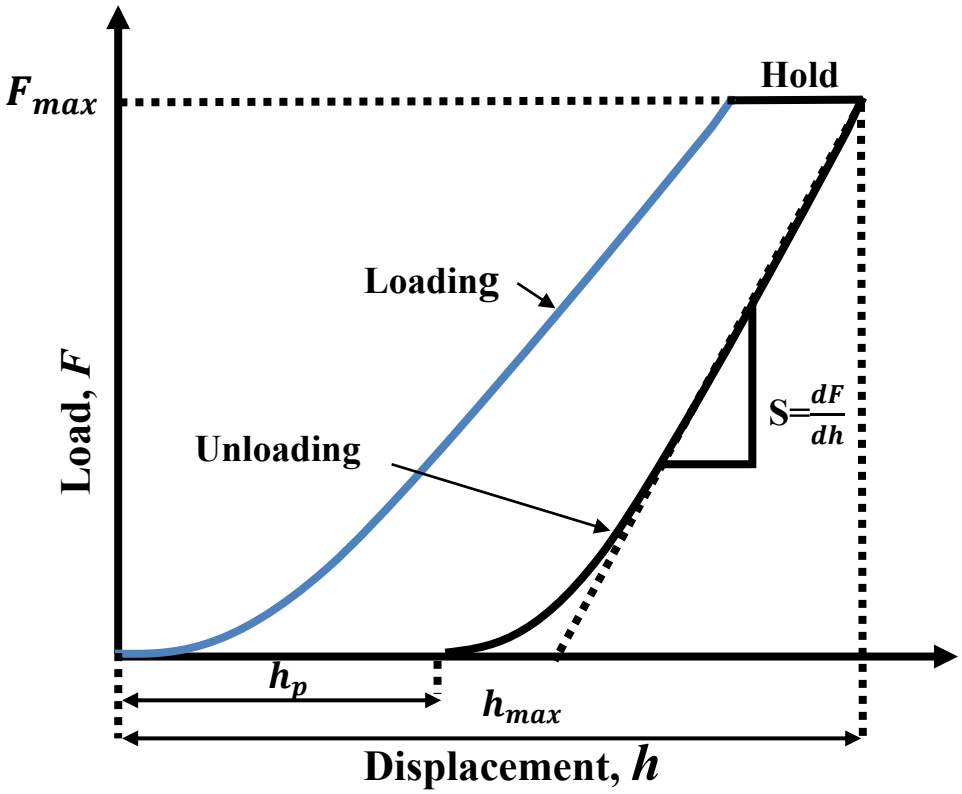

Fig. 2. A derived load-displacement curve from an instrumented indentation test adapted from Ref [11,22].

Based on the load-displacement profile, a reduced elastic modulus (E_r) is obtained from the projected contact area and computed unloading stiffness (S) as shown in Eq. 1 [22,32]:

$$E_r = \frac{\sqrt{\pi}}{2\beta}\frac{S}{\sqrt{A_c}} \tag{1}$$

where $S = \left(\frac{dF}{dh}\right)_{unloading}$, β is a correction factor for the shape of the indenter tip, which is dimensionless. β=1.05 is used frequently for a Berkovich indenter. A_c is the projected contact area between the sample and indenter that can be obtained solely using indentation parameters [22,32]. The projected contact area for an indenter tip is given by Eq. [32]):

$$A_c = f h_c^2 \tag{2}$$

where f is the area function, which depends on the indenter geometry and the magnitude of the specimen. For an ideal Berkovich diamond indenter, which is commonly used, the value of f is taken as 24.56 [32].

The reduced elastic modulus incorporates bi-directional displacements in both contacting bodies i.e., the indenter and sample to be tested, and is related to the elastic modulus, E, through the Eq. 3 [22,32]:

$$\frac{1}{E_r} = \frac{1 - V^2}{E} + \frac{1 - V_i^2}{E_i} \tag{3}$$

where V and V_i are Poisson's ratio of the sample and indenter, E and E_i are the elastic modulus of the sample and indenter, respectively.

Using the values of a given diamond indenter, E_i = 1141 GPa and V_i = 0.07 [21], the elastic modulus, E for a test specimen can therefore be computed using Eq. 4:

$$E = (1 - V^2)\left[\frac{1}{E_r} - \frac{1 - V_i^2}{E_i}\right]^{-1} \tag{4}$$

It is of note that the elastic modulus equation takes into cognizance the elastic deformations, which occurs in the indenter and sample. Even though Eq. 4 was initially proposed for elastic solids, it has been shown in recent times to be valid for elastic-plastic solids [33]. Furthermore, it has been shown that small perturbations on the geometry of the indenter do not influence the outcome of the elastic modulus [34]. Meanwhile, the hardness (H) of the test sample is computed as the ratio of the maximal indentation load (F_{max}) to the projected contact area (A_c), expressed as Eq. 5 [22,32]:

$$H = \frac{F_{max}}{A_c} \tag{5}$$

IIT enhances indentation techniques by indenting at a nanoscale, as against other micro or macro techniques, using a very accurate tip shape, high structural resolutions to capture the indents, and as such produce real-time data for the load-displacement curve during the indentation process [14]. When this nanoindentation technique is compared to other mechanical test methods in the micrometer range, it is relatively easy to setup and sample preparation is less complicated [35]. Another great advantage of IIT is that the projected contact area can most at times be derived from the continuous load-displacement data alone [22,32]. This implies that the impression of the residual hardness does not have to be imaged directly and measurement of the properties at the micrometer scale are, therefore, facilitated. These advantages enable the use of the nanoindentation technique to test oil shale cuttings or sidewalls of wellbore samples obtained from conventional drilling operations and are less expensive than core samples.

3 Materials and method

3.1 Characterization of the shale cuttings

Side wall shale cuttings were obtained from two different deviated depths (9000 ft. and 10500 ft., herein referred to as FT9000 and FT10500) in a wellbore within the Niger-Delta region of Nigeria. The shale cuttings used for the IIT measurements were mounted and the sample surfaces were mechanically polished with increasing grit sizes of SiC paper up to a final grade of 1200. Fig. 3 shows samples of the shales polished and the SiC abrasive papers used. This was done to achieve a relatively smooth surface before characterizing them. X-ray Diffraction (XRD) analysis was performed on the samples using a Benchtop X-ray Diffraction (XRD)

analyser (Bruker BV 2D PHASER model) with a copper $K\alpha_1$ radiation source (λ= 0.1542 nm) at 30 kV and 10 mA with 2θ reflection geometry, values varying between 5^0 - 90^0 with a step size of 0.0568^0 during the phase identification measurement. A Zeiss Ultra Plus 55 model Field Emission Scanning Electron Microscope (FE-SEM) set at 2.0 kV was utilized to image and examine the microstructure of the shale cuttings.

3.2 Instrumented Indentation Testing (IIT) of the shale cuttings

Nanoindentation tests were performed on the polished shale specimen using the Hysitron (model TI 750H Ubi) nanoindenter at Sheda Science and Technology Complex, FCT, Nigeria. A Berkovich indenter with tip dimensions (radius - 100 nm and apex - 70.3^o) was used for the measurement. The samples were indented at two peak loads (PL) of 5000 and 7000 µN, respectively. The load-time sequence was 5 seconds for loading, 3 seconds for holding at the peak loads, then 5 seconds for unloading process consistent with the methodology outline [32].

Indents were inscribed at various locations on each of the sample using the same load-time sequence. The distance between these indents was about 100 µm apart to prevent any form of interference between them. The results obtained from these tests were then averaged for each value of the mechanical properties of interest (hardness and elastic modulus).

Fig. 3. (a) Shale samples mounted and (b) polished with 400 – 1200 grit SiC abrasive papers.

4 Results and discussions

4.1 Morphological and structural characterization

The XRD result shows the mineral composition within the shales. The sharp XRD peaks in Fig. 4 suggest the presence of crystalline mineral phases. Typical quartz (SiO_2) with sharp peaks is observed irrespective of the depth of the shale formation. The other diffraction peaks seen in both samples signify the presence of other minerals in the shale, which include magnetite, kaolinite, alumina, feldspar and calcite in agreement with previous studies [16,26]. However, as we move down in depth, the presence of magnetite and feldspar are seen to reduce, which can be seen from the almost absent peak in the FT10500 sample. This could be attributed to the mineral variability of shales that varies across depths and locations, which in turn is most likely to influence the mechanical parameters of the shale materials in this region.

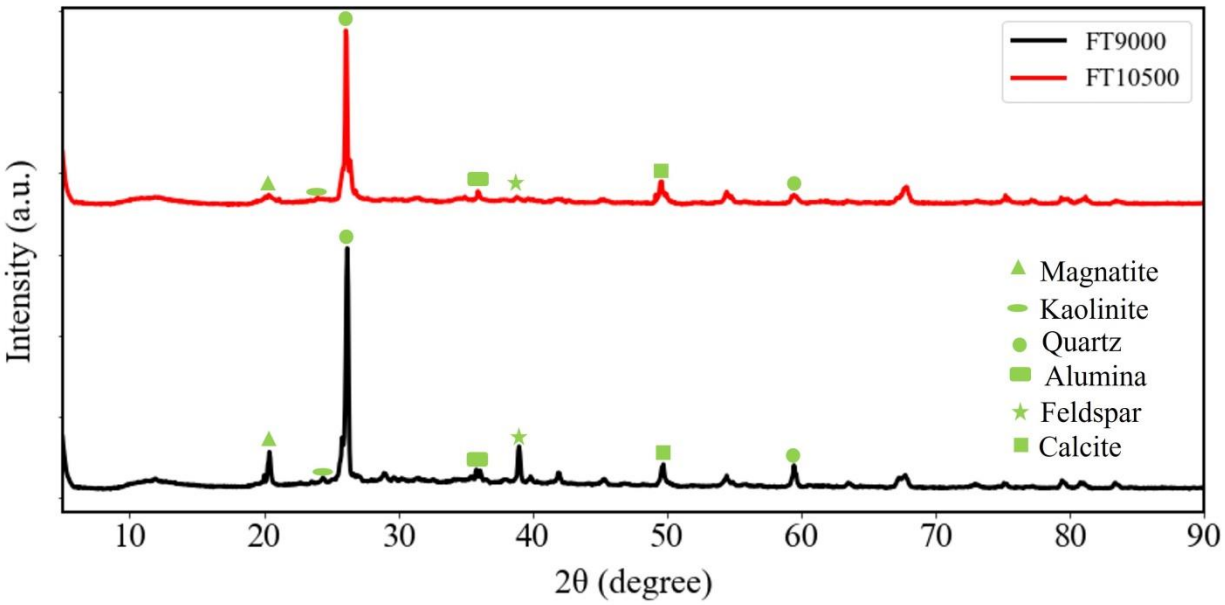

Fig. 4. XRD pattern of the shale samples at a depth of 10500 and 9000 ft., respectively.

SEM results as seen in Fig. 5, gives further insight into the morphology associated with this shale type. The images at low and high magnification reveal a network of various minerals and organic matters, which consist of interparticle and intraparticle pores with sizes from the order of micrometer to the nanometer length scale. The bonding of both matters forms a composite structure which accounts for the ability of shales to accommodate hydrocarbons within their structure during rock pyrolysis [16]. Despite the interlayer bonding, there are still some forms of heterogeneity associated with these shales. The SEM results show variations in their structural properties, which include variations in the mineralogy and organic matter distribution. In the FT9000 shale sample, finer and more orderly layered mineral and organic matters can be seen, as compared to the coarse distribution of these constituent matters in the FT10500 sample. This confirms the heterogeneity commonly associated with shales across varied depths and layers [9,11,16].

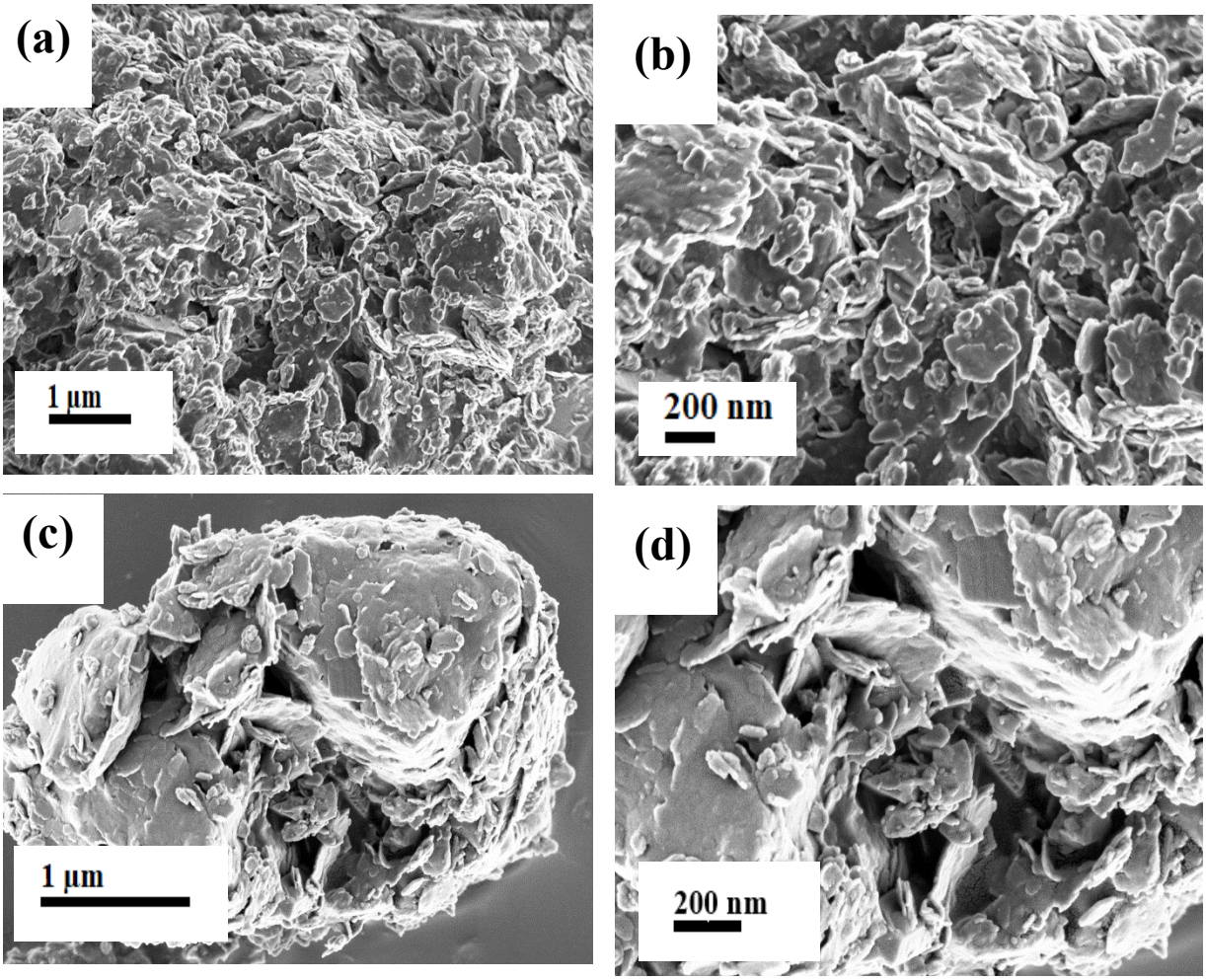

Fig. 5. The morphology of the shale sample at (a, b) 10500 and (c, d) 9000 ft. respectively. Large intergranular and smaller intragranular pores are observed in both samples at a magnification of 1µm and 200 nm.

4.2 Mechanical property measurements

The load-displacement curve for the test samples at a peak load (PL) of 5000 µN (Fig. 6) shows the constantly changing load and penetration depths measured simultaneously during the test. By implication, it shows the extent of the deformation of the samples for the entire period the load is in contact with it. It also indicates the possibility of measuring the deformation of a shale formation as pressure is applied during drilling operations or any other activities.

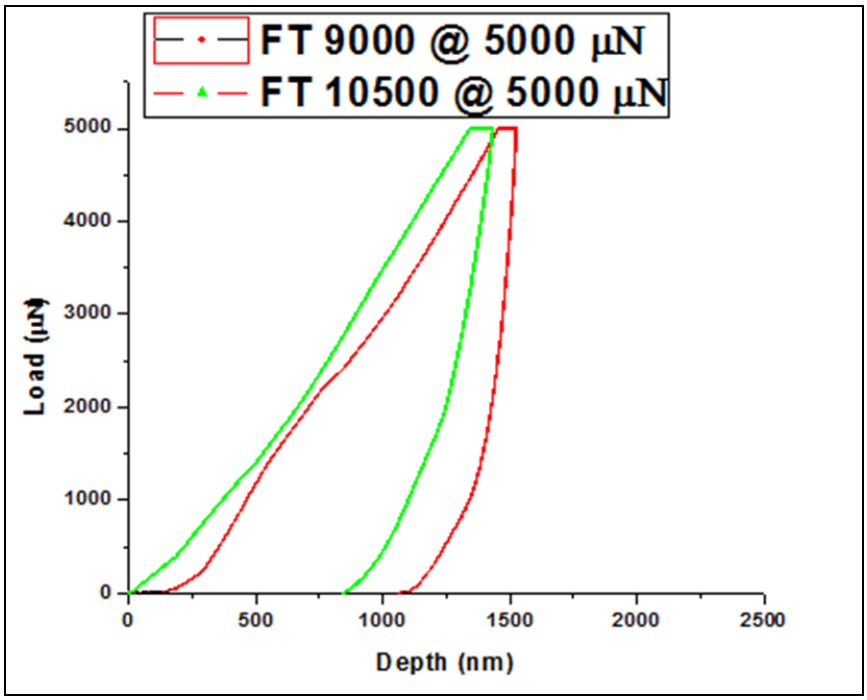

Fig. 6. Load-depth curves obtained from the indentation experiment at a peak load of 5000 µN.

With the aid of a Triboscan analysis software, reduced modulus values were obtained from analyzing the load-depth curves. The hardness and elastic modulus of the shale samples were computed using Eqs. 1-5. The obtained mechanical properties for the shales tested are shown in Table 1. It can be observed that their properties varied with the well depths and applied indentation loads.

Table 1 Measured mechanical properties of oil shale cutting samples.

Sample	Reduced Elastic Modulus, E_r (GPa)		Elastic Modulus, E (GPa)		Hardness, H (MPa)	
	5000 µN	7000 µN	5000 µN	7000 µN	5000 µN	7000 µN
FT9000	5.00 ± 0.18	5.46 ± 0.19	4.70 ± 0.16	5.14 ± 0.20	85.42 ± 3.80	52.12 ± 1.80
FT10500	2.85 ± 0.10	4.26 ± 0.15	2.66 ± 0.13	4.01 ± 0.10	109.26 ± 5.10	102.24 ± 4.70

For comparison, these results have been represented in the charts shown in Fig. 7. It would be observed that the PL1 (indentation load of 5000 µN) yielded relatively higher values for the hardness property of the shale samples but relatively lower values for their elastic modulus. This disparity is traceable to the heterogeneity of shales and as such the average value from the two indentations was rather used as shown in Fig. 8. Also, the hardness of the oil shales ranged from 68.77 ± 2.80 MPa to 105.75 ± 4.90 MPa, while the elastic modulus was between 3.36 ± 0.18 GPa to 4.92 ± 0.12 GPa.

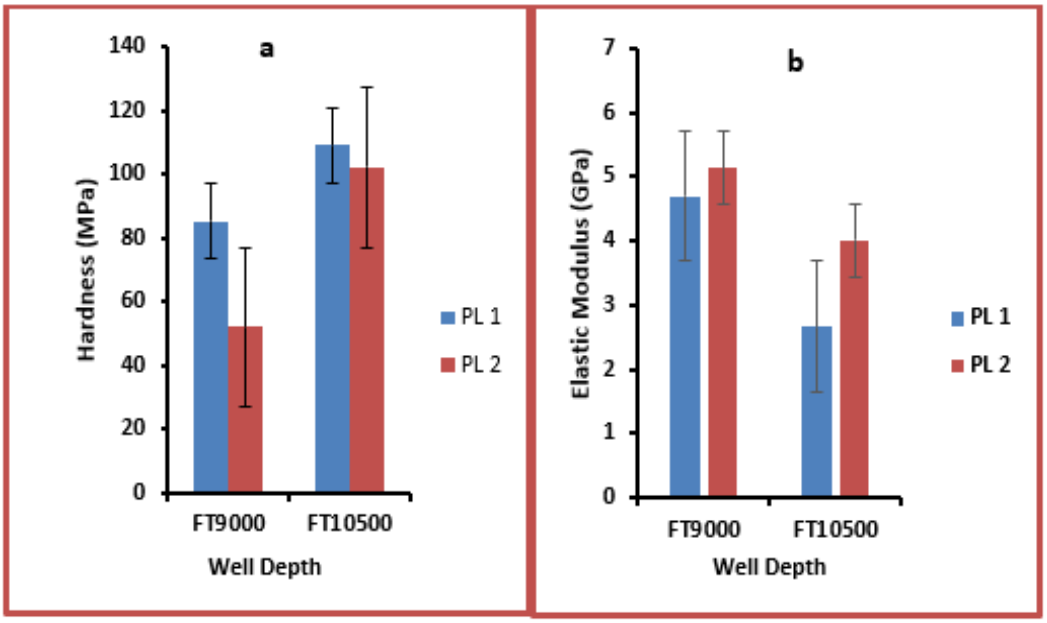

Fig. 7. Mechanical property measurements of shale specimen at different well depths based on peak loads of 5000 μN and 7000 μN (as PL 1 and PL 2 respectively) - (a) hardness and (b) elastic modulus.

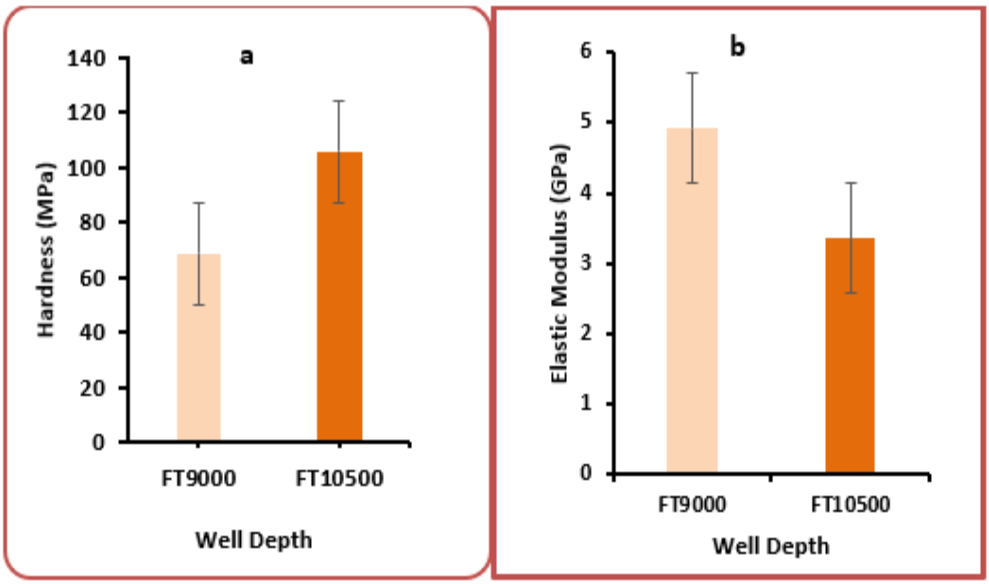

Fig. 8. Average (a) hardness and (b) elastic modulus at different well depths.

We see from the outcome of the study that the hardness of the Niger Delta shales increases with their well depths. This lends credence to why it is usually difficult to fracture through a shale formation while drilling down the wellbore. Therefore, it will require more water, sand, and chemicals such as hydrochloric acid, sodium chloride, magnesium oxide, etc., to break through the formation. The mechanical property measurements of the shales so obtained can also be used to determine the hydrocarbon storage capacity of their formations and wellbore stability.

5 Conclusions

The characterization and measurements of shales are important to establish their strength and behavior under downhole conditions in order to enhance wellbore stability and optimize drilling operations. Mechanical properties of shales, such as; hardness, elastic modulus and unconfined compressive strength, are important parameters in determining the hydrocarbon storage space and hydraulic fracturing optimization of unconventional shale reservoirs in order to improve the production level. Due to the extensive heterogeneity of oil shale formations across depths and locations, a focused study of oil shale cuttings obtained from the sidewalls of two different depths in a wellbore in the Niger Delta region of Nigeria was performed. Insight into the morphology of these shales was established in this study. The results obtained from the SEM image showed an interlayers of the mineral and organic matters, which account for the possibility of hydrocarbons within the structure. In addition, the result also revealed the heterogeneity associated with these shales across varied depths and layers.

Furthermore, essential mechanical properties of these Niger Delta shales, elastic modulus and hardness, were obtained from the shale cuttings using the IIT technique. This method is significantly effective in terms of cost and production time when compared to using conventional standard tests. The measure hardness values of the shales ranged from 68.77 ± 2.80 MPa to 105.75 ± 4.90 MPa, while the elastic modulus range from 3.36 ± 0.18 GPa to 4.92 ± 0.12 GPa. The study also shows that the hardness of these shales increase with their well depths, which further explains the difficulty usually encountered when fracturing through a shale formation. The test procedure can also be extended to obtain other mechanical properties such as interfacial adhesion and fracture toughness.

Acknowledgements

The authors expressed gratitude to the laboratory team at the Physics Advanced Research Centre of Sheda Science and Technology Complex, Nigeria, where the instrumented indentation test was conducted. Equally, we would like to appreciate Dr. Kabiru Oyedotun for assisting with the SEM and XRD tests at the University of Pretoria, South Africa. We are also grateful to Dr. Alpheus Igbokoyi of the Petroleum Engineering Department, African University of Science and Technology, Abuja, Nigeria for his support towards this research work.

References

[1] J. Taheri-shakib, A. Kantzas, Review article A comprehensive review of microwave application on the oil shale : Prospects for shale oil production, Fuel. 305 (2021) 121519. https://doi.org/10.1016/j.fuel.2021.121519.

[2] R.P. Steiger, P.K. Leung, Quantitative determination of the mechanical properties of shales, SPE Driilling Eng. 7 (1992) 181–185. https://doi.org/10.2118/18024-PA.

[3] G. Chen, M.E. Chenevert, M.M. Sharma, M. Yu, A study of wellbore stability in shales including poroelastic , chemical , and thermal effects, J. Pet. Sci. Eng. 38 (2003) 167–176. https://doi.org/10.1016/S0920-4105(03)00030-5.

[4] J. Hay, C.H. Sondergeld, Mechanical Testing of Shale by Instrumented Indentation, Agil. Technol. Appl. Note. (2010) 1–8.

[5] P. Horsrud, Estimating mechanical properties of shale from empirical correlations, SPE Drill. Complet. 16 (2001) 68–73. https://doi.org/10.2118/56017-PA.

[6] P. Chen, Q. Han, T. Ma, D. Lin, The mechanical properties of shale based on micro-indentation test, Pet. Explor. Dev. 42 (2015) 723–732. https://doi.org/10.1016/S1876-3804(15)30069-0.

[7] X. Niu, D. Yan, M. Hu, Z. Liu, X. Wei, M. Zuo, Controls of distinct mineral compositions on pore structure in over-mature shales: A case study of lower Cambrian niutitang shales in South China, Minerals. 11 (2021) 1–19. https://doi.org/10.3390/min11010051.
[8] X. Wang, J. Hou, S. Li, L. Dou, S. Song, Q. Kang, D. Wang, Insight into the nanoscale pore structure of organic-rich shales in the Bakken Formation, USA, J. Pet. Sci. Eng. 191 (2020) 107182. https://doi.org/10.1016/j.petrol.2020.107182.
[9] Y. Wang, L. Liu, S. Zheng, Z. Luo, Y. Sheng, X. Wang, Full-scale pore structure and its controlling factors of the Wufeng-Longmaxi shale , southern Sichuan Basin , China : Implications for pore evolution of highly overmature marine shale, J. Nat. Gas Sci. Eng. 67 (2019) 134–146. https://doi.org/10.1016/j.jngse.2019.04.020.
[10] Y. Wang, Y. Zhu, S. Liu, R. Zhang, Pore characterization and its impact on methane adsorption capacity for organic-rich marine shales, Fuel. 181 (2016) 227–237. https://doi.org/10.1016/j.fuel.2016.04.082.
[11] A. Akono, Nano-scale characterization of organic-rich shale via indentation methods, in: New Front. Oil Gas Explor., Springer International Publishing Switzerland, 2016: pp. 209–233. https://doi.org/10.1007/978-3-319-40124-9.
[12] L.L. Wang, D.S. Yang, R.W. Yang, S. Chanchole, Investigating the mechanical behavior of shale: A micro-scale approach, J. Nat. Gas Sci. Eng. 36 (2016) 1295–1302. https://doi.org/10.1016/j.jngse.2016.03.051.
[13] D.J.K. Ross, R. Marc Bustin, The importance of shale composition and pore structure upon gas storage potential of shale gas reservoirs, Mar. Pet. Geol. 26 (2009) 916–927. https://doi.org/10.1016/j.marpetgeo.2008.06.004.
[14] K. Liu, M. Ostadhassan, B. Bubach, Applications of nano-indentation methods to estimate nanoscale mechanical properties of shale reservoir rocks, J. Nat. Gas Sci. Eng. 35 (2016) 1310–1319. https://doi.org/10.1016/j.jngse.2016.09.068.
[15] T. Saif, Q. Lin, B. Bijeljic, M.J. Blunt, Microstructural imaging and characterization of oil shale before and after pyrolysis, Fuel. 197 (2017) 562–574. https://doi.org/10.1016/j.fuel.2017.02.030.
[16] B. Hazra, A.K. Varma, A.K. Bandopadhyay, S. Chakravarty, J. Buragohain, S.K. Samad, A.K. Prasad, FTIR, XRF, XRD and SEM characteristics of Permian shales, India, J. Nat. Gas Sci. Eng. 32 (2016) 239–255. https://doi.org/10.1016/j.jngse.2016.03.098.
[17] P. Sarkar, K.H. Singh, Petrophysical Characterization of Gondwana Shales of South Karanpura Coal Field, Jharkhand, India, ASEG Ext. Abstr. 2016 (2016) 1–8. https://doi.org/10.1071/aseg2016ab248.
[18] D. Lai, G. Zhang, G. Xu, Characterization of oil shale pyrolysis by solid heat carrier in moving bed with internals, Fuel Process. Technol. 158 (2017) 191–198. https://doi.org/10.1016/j.fuproc.2017.01.005.
[19] P. Shukla, V. Kumar, M. Curtis, C.H. Sondergeld, C.S. Rai, Nanoindentation studies on shales, in: 47th US Rock Mech. / Geomech. Symp. 2013, ARMA-2013-578, 2013: pp. 1194–1203.
[20] G. Dong, P. Chen, A comparative experiment investigate of strength parameters for Longmaxi shale at the macro- and mesoscales, Int. J. Hydrogen Energy. 42 (2017) 20082–20091. https://doi.org/10.1016/j.ijhydene.2017.05.240.
[21] W.C. Oliver, G.M. Pharr, An improved technique for determining the hardness and elastic modulus using load and dislacemnet sensing indentation experiments, J. Mater. Res. 7 (1992) 1564–1583. https://doi.org/10.1557/JMR.1992.1564.
[22] W.C. Oliver, G.M. Pharr, Measurement of hardness and elastic modulus by instrumented

indentation: Advances in understanding and refinements to methodology, J. Mater. Res. 19 (2004) 3–20. https://doi.org/10.1089/neu.2017.5398.
[23] W.C. Pethica, J.B., Hutchings, R. and Oliver, Hardness measurement at penetration depths as small as 20 nm, Philos. Mag. A. 48 (1983) 593–606. https://doi.org/https://doi.org/10.1080/01418618308234914.
[24] M.F. Doerner, W.D. Nix, A method for interpreting the data from depth-sensing indentation instruments, J. Mater. Res. 1 (1986) 601–609. https://doi.org/10.1557/JMR.1986.0601.
[25] F.E. Oboh, Middle Miocene palaeoenvironments of the Niger Delta, Palaeogeogr. Palaeoclimatol. Palaeoecol. 92 (1992) 55–84. https://doi.org/10.1016/0031-0182(92)90135-R.
[26] D.O. Lambert-Aikhionbare, H.F. Shaw, Significance of clays in the petroleum geology of the Niger Delta, Clay Miner. 17 (1982) 91–103. https://doi.org/10.1180/claymin.1982.017.1.09.
[27] R.W. Wiener, M.G. Mann, M.T. Angelich, J.B. Molyneux, Mobile shale in the Niger Delta: Characteristics, structure, and evolution, AAPG Mem. (2010) 145–161. https://doi.org/10.1306/13231313M933423.
[28] E.U. Okpogo, C.P. Abbey, I.O. Atueyi, Reservoir characterization and volumetric estimation of Orok Field, Niger Delta hydrocarbon province, Egypt. J. Pet. 27 (2018) 1087–1094. https://doi.org/10.1016/j.ejpe.2018.03.014.
[29] O.O. Osinowo, J.O. Ayorinde, C.P. Nwankwo, O.M. Ekeng, O.B. Taiwo, Reservoir description and characterization of Eni field Offshore Niger Delta, southern Nigeria, J. Pet. Explor. Prod. Technol. 8 (2018) 381–397. https://doi.org/10.1007/s13202-017-0402-7.
[30] I. Olorunniwo, S.J. Olotu, O.A. Alao, A.A. Adepelumi, Hydrocarbon reservoir characterization and discrimination using well-logs over " AIB-EX " Oil Field , Niger Delta., Heliyon. 5 (2019) e01742. https://doi.org/10.1016/j.heliyon.2019.e01742.
[31] D.K. Oyeyemi, M.T. Olowokere, A.P. Aizebeokhai, Hydrocarbon resource evaluation using combined petrophysical analysis and seismically derived reservoir characterization, offshore Niger Delta, J. Pet. Explor. Prod. Technol. 8 (2018) 99–115. https://doi.org/10.1007/s13202-017-0391-6.
[32] J. Hay, Introduction to instrumented indentation testing, Exp. Tech. 33 (2009) 66–72. https://doi.org/10.1111/j.1747-1567.2009.00541.x.
[33] C.-M. Cheng, Y.-T. Cheng, On the initial unloading slope in indentation of elastic-plastic solids by an indenter with axisymmetric smooth profile, Appl. Phys. Lett. 71 (1997) 2623. https://doi.org/https://doi.org/10.1063/1.120159.
[34] H. Gao, T.-W. Wu, A note on the elastic contact stiffness of a layered medium, J. Mater. Res. 8 (1993) 3229–3232. https://doi.org/https://doi.org/10.1557/JMR.1993.3229.
[35] B. Poon, D. Rittel, G. Ravichandran, An analysis of nanoindentation in linearly elastic solids, Int. J. Solids Struct. 45 (2008) 6018–6033. https://doi.org/10.1016/j.ijsolstr.2008.07.021.